A Relaxation-Compensated Carr−Purcell−Meiboom−Gill Sequence for Characterizing Chemical Exchange by NMR Spectroscopy

J. Patrick Loria,[†] Mark Rance,*,[‡] and Arthur G. Palmer III*,[†]

Department of Biochemistry and Molecular Biophysics
Columbia University, New York, New York 10032
Department of Molecular Genetics
Biochemistry, and Microbiology
University of Cincinnati, Cincinnati, Ohio 45267

Functions of biological macromolecules, including enzyme catalysis, allostery, and ligand recognition, in some circumstances can be rate-limited by dynamic processes that couple nonproductive and productive conformations.[1,2] Delineating the amplitudes, rates, and mechanisms of these motions is necessary to explicate biological function.[3−5] This paper describes a modified proton-detected [15]N Carr−Purcell−Meiboom−Gill[6,7] (CPMG) spin−echo pulse sequence that overcomes the disadvantages associated with pulsing rates comparable to the one-bond J_{NH} scalar coupling constant. The new experiment permits measurement of chemical or conformational exchange time constants from approximately 0.5 to 5 ms. This range of time scales fills an important gap between microsecond time scales that are accessible by the off-resonance rotating-frame experiment[8,9] and millisecond time scales that are accessible by the *zz*-exchange experiment.[10−12]

Conformational or chemical kinetic processes that transfer a nuclear spin between sites with different magnetic environments contribute to the adiabatic decay of transverse magnetization. The phenomenological transverse relaxation rate constant measured in a CPMG experiment, $R_2(\tau_{cp})$, is given by:

$$R_{2(\tau_{cp})} = \epsilon R_{in} + (1 - \epsilon)R_{anti} + R_{ex} \tag{1}$$

in which τ_{cp} is the delay between pulses in the spin−echo pulse train; R_{in} and R_{anti} are the transverse relaxation rate constants for in-phase and antiphase coherences averaged over the populations of each chemical or conformational state, respectively; $0 \leq \epsilon \leq 1$ reflects the averaging between in-phase and antiphase coherences due to evolution under the scalar coupling Hamiltonian during τ_{cp};[13−15] and R_{ex} is the rate constant for damping due to

(1) Frauenfelder, H.; Sligar, S. G.; Wolynes, P. G. *Science* **1991**, *254*, 1598−1603.
(2) Karplus, M.; McCammon, J. A. *Annu. Rev. Biochem.* **1983**, *53*, 263−300.
(3) Williams, J. C.; McDermott, A. E. *Biochemistry* **1995**, *34*, 8309−8319.
(4) Kay, L. E. *Nat. Struct. Biol.* **1998**, *5*, 513−517.
(5) Palmer, A. G. *Curr. Opin. Struct. Biol.* **1997**, *7*, 732−737.
(6) Carr, H. Y.; Purcell, E. M. *Phys. Rev.* **1954**, *94*, 630−638.
(7) Meiboom, S.; Gill, D. *Rev. Sci. Instrum.* **1958**, *29*, 688−691.
(8) Akke, M.; Palmer, A. G. *J. Am. Chem. Soc.* **1996**, *118*, 911−912.
(9) Zinn-Justin, S.; Berthault, P.; Guenneugues, M.; Desvaux, H. *J. Biomol. NMR* **1997**, *10*, 363−372.
(10) Montelione, G. T.; Wagner, G *J. Am. Chem. Soc.* **1989**, *111*, 3096−3098.
(11) Wider, G.; Neri, D.; Wüthrich, K. *J. Biomol. NMR* **1991**, *1*, 93−98.
(12) Farrow, N.; Zhang, O.; Forman-Kay, J. D.; Kay, L. E. *J. Biomol. NMR* **1994**, *4*, 727−734.
(13) Gutowsky, H. S.; Vold, R. L.; Wells, E. J. *J. Chem. Phys.* **1965**, *43*, 4107−4125.
(14) Palmer, A. G.; Skelton, N. J.; Chazin, W. J.; Wright, P. E.; Rance, M. *Mol. Phys.* **1992**, *75*, 699−711.
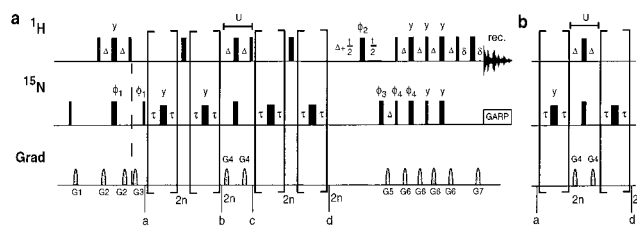
Figure 1. Relaxation-compensated CPMG pulse sequences for measuring conformational and chemical exchange. All pulses are *x* phase unless otherwise indicated. Narrow and wide bars depict 90 and 180° pulses, respectively. The 180° [15]N pulses in the spin−echo sequence had durations of 97 μs. Delays are Δ = 2.7 ms, τ = 0.5 τ_{cp}, and δ = 200 μs. Decoupling during acquisition used GARP phase modulation with a field strength of 1000 Hz. The phase cycle is $\phi_1 = x, -x$; $\phi_2 = 4(x), 4(-x)$; $\phi_3 = x, x, y, y, -x, -x, -y, -y$; $\phi_4 = y$; receiver = $x, -x, -x, x$. The gradient pulses had the shape of the center lobe of a sine function. Gradient durations G1−G7 were 1 ms, 0.4 ms, 3 ms, 0.5 ms, 1.8 ms, 0.6 ms, 0.184 ms. Gradient amplitudes were $G1_{xyz}$ = 10 G/cm; $G2_{xyz}$ = 7 G/cm; $G3_z$ = 34 G/cm; $G4_{xyz}$ = 8 G/cm; $G5_{xyz}$ = 28 G/cm; $G6_z$ = 14 G/cm; and $G7_{xyz}$ = 28 G/cm. Coherence selection was achieved by inverting the amplitude of $G5$ and phase ϕ_4; the receiver phase and ϕ_1 were inverted for each t_1 increment.[22,23] The inset (b) shows a modification of the pulse sequence used to measure $R_2(\tau_{cp})$ for longer τ_{cp} values.

exchange between sites. For two exchanging sites[16]

$$R_{ex} = \Phi_{ex}\tau_{ex}[1 - (2\tau_{ex}/\tau_{cp})\tanh(\tau_{cp}/2\tau_{ex})] \tag{2}$$

in which $\Phi_{ex} = (\omega_1 - \omega_2)^2 p_1 p_2$; and p_i and ω_i are the populations and Larmor frequencies for the nuclear spin in site *i*; and τ_{ex} is the reduced lifetime of the exchanging sites.

In principle, exchange kinetics can be determined by fitting eqs 1 and 2 to $R_2(\tau_{cp})$ data obtained for different values of τ_{cp}; however, both ϵ and R_{ex} depend on τ_{cp}, which renders the analysis intractable. This difficulty is circumvented if τ_{cp} is limited to small values ($<1/(4J_{NH})$), because $\epsilon \approx 1$.[17] In this case, only fast exchange processes can be studied, and the resulting high radio frequency duty cycle poses a significant drawback compared with the off-resonance rotating-frame experiment.[8,9] Broadband proton decoupling during τ_{cp} prevents evolution of in-phase into antiphase magnetization and makes $\epsilon = 1$; however, decoupling interferes with spin−echo formation and accentuates the decay of transverse magnetization.[14,15,18] In the approach adopted herein, the rate constants for in-phase and antiphase coherences are averaged explicitly during the CPMG sequence to render $\epsilon = 0.5$ for all τ_{cp}. Application of the experiment to basic pancreatic trypsin inhibitor (BPTI) confirms the effectiveness of the proposed averaging procedure for values of τ_{cp} as large as $2/J_{NH}$.

The modified CPMG pulse sequence is shown in Figure 1. At point a, the density operator is proportional to $2I_zS_y$ ($I = $ [1]H and $S = $ [15]N spin operators). Between points a and b, the relaxation of the density operator is described by eq 1 with $\epsilon = \epsilon_{ab} = 0.5$ $[1 - \text{sinc}[\pi J_{NH}\tau_{cp}]]$.[14] The period **U** converts antiphase $2I_zS_y$ coherence to in-phase S_x coherence at point c, and the [1]H 90° pulse at the end of **U** purges any residual antiphase magnetization. Between points c and d, the relaxation of the density operator is described by eq 1 with $\epsilon = \epsilon_{cd} = 0.5$ $[1 + \text{sinc}[\pi J_{NH}\tau_{cp}]]$. The [1]H 180° pulses midway between points a and b and between points c and d suppress CSA/dipolar relaxation interference.[14,15] The time

(15) Kay, L. E.; Nicholson, L. K.; Delaglio, F.; Bax, A.; Torchia, D. A. *J. Magn. Reson.* **1992**, *97*, 359−375.
(16) Allerhand, A.; Thiele, E. *J. Chem. Phys.* **1966**, *45*, 902−916.
(17) Orekhov, V. Y.; Pervushin, K. V.; Arseniev, A. S. *Eur. J. Biochem.* **1994**, *219*, 887−896.
(18) Shaka, A. J.; Keeler, J. *Prog. Nucl. Magn. Reson. Spectrosc.* **1987**, *19*, 47−129.
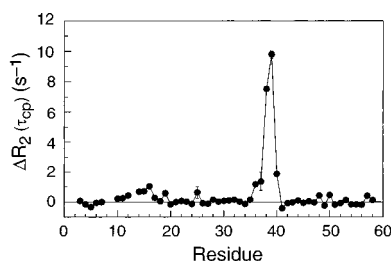
Figure 2. Conformational exchange in BPTI. The differences $\Delta R_2(\tau_{cp})$ = $R_2(10$ ms$)$ − $R_2(1$ ms$)$ are plotted versus the residue number. Uncertainties usually are smaller than the size of the data points. Data were recorded on a 2.6 mM [U-98% ^{15}N] BPTI sample (pH = 5.1, T = 300 K) using a Bruker DRX500 NMR spectrometer with a ^{15}N Larmor frequency of 50.68 MHz. Spectra were acquired using (180 × 4096) complex points and spectral widths of (2500 × 12500) Hz in the (t_1 × t_2) dimensions. The recycle delay was 3 s and a total of 16 transients were recorded for each complex t_1 point. Relaxation decay curves were measured for eight values of τ_{cp} ranging from 1 to 20 ms. From 10 to 15 relaxation time points (including duplicates) were acquired for each decay curve by varying n in Figure 1. Uncertainties in the relaxation rate constants were obtained from jackknife simulations.[24]

decay of the magnitude of the density operator between points a and d is given by

$$I(8n\tau_{cp}) = I_0 \exp[-4n\tau_{cp}(\epsilon_{ab}R_{in} + \{1 - \epsilon_{ab}\}R_{anti} + R_{ex})] \times$$
$$\exp[-4n\tau_{cp}(\epsilon_{cd}R_{in} + \{1 - \epsilon_{cd}\}R_{anti} + R_{ex})]$$
$$= I_0 \exp[-8n\tau_{cp}(\bar{R} + R_{ex})] \qquad (3)$$

in which n ≥ 0 is an integer, $\bar{R} = 0.5 (R_{in} + R_{anti})$, and the transfer efficiency of **U** is incorporated into I_0. Thus, the effective $R_2(\tau_{cp})$ = $\bar{R} + R_{ex}$. After point d, the magnetization is frequency labeled during t_1 and transferred to the I spins for detection. The modification of the pulse sequence shown in Figure 1b reduces the minimum increment between time points from $8\tau_{cp}$ to $4\tau_{cp}$, which facilitates measurements using long τ_{cp} values. In this sequence, **U** serves the dual role of interchanging in-phase and antiphase magnetization and suppressing CSA/dipolar interference; however, the suppression is not as efficient as in Figure 1a.

The relaxation-compensated CPMG experiment was performed on a 2.6 mM [U-98% ^{15}N] BPTI sample at 300 K;[19] other experimental conditions are given in the caption to Figure 2. The differences between $R_2(\tau_{cp})$ measured at τ_{cp} values of 10.0 and 1.0 ms for BPTI are presented in Figure 2. No significant differences in relaxation rate constants are observed for the majority of the backbone ^{15}N spins, which confirms the robustness of the averaging procedures incorporated into the pulse sequences. Differences between the two experiments are observed for residues in the vicinity of C14 and C38. The relaxation dispersion curves for residues C14, Q31, C38, R39 are shown in Figure 3. Residue Q31 is typical of those residues in BPTI that do not exhibit τ_{cp}-dependent dispersion and are not subject to conformational exchange. Q31 has a mean value of $R_2(\tau_{cp}) = \bar{R} = 7.4 \pm 0.2$ s^{-1} which agrees with $\bar{R} \approx 7.2$ s^{-1} estimated for a rotational correlation time of 3 ns. A pronounced dependence of $R_2(\tau_{cp})$ on τ_{cp} is observed for C38 and C39; smaller amplitude dispersion was observed for residues A16, G36, G37, and A40. The results for $\bar{R}$, Φ_{ex}, and τ_{ex} obtained from the $R_2(\tau_{cp})$ data are given in Table 1. C14 has an average value of $R_2(\tau_{cp}) = 10.6 \pm 0.3$ s^{-1}, which is greater than expected for $\bar{R}$, but does not exhibit any dependence on τ_{cp}; similar results are obtained for K15. Thus, these residues are subject to conformational exchange on time scales <0.5 ms that are not accessible to the present technique.
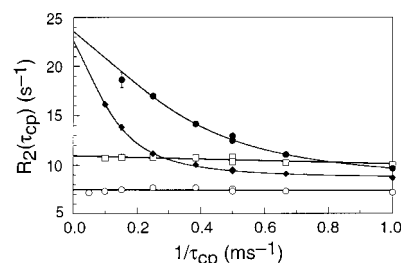
Figure 3. CPMG dispersion curves for BPTI. Values of $R_2(\tau_{cp})$ are plotted versus $1/\tau_{cp}$ for C14 (□), Q31 (○), C38 (◆), and R39 (●). Solid lines for C38 and R39 are the best fits to eqs 1 and 2; fitted parameters are given in Table 1. The solid lines for C14 and Q31 are drawn at the mean value of $R_2(\tau_{cp})$ and are only meant to guide the eye. The pulse sequence of Figure 1a was used for most experiments; a duplicate data set at $1/\tau_{cp} = 0.5$ ms^{-1} and all data for $1/\tau_{cp} \leq 0.1$ ms^{-1} were obtained using the pulse sequence shown in Figure 1b.

Table 1. Conformational Exchange Parameters for BPTI

residue	τ_{ex} (ms)	$\Phi_{ex}\tau_{ex}$ (sec^{-1})	$\bar{R}$ (sec^{-1})
A16	4.52 ± 0.22	3.36 ± 0.10	6.61 ± 0.03
G36	3.42 ± 0.28	2.82 ± 0.15	8.98 ± 0.04
G37	3.21 ± 0.63	3.90 ± 0.72	8.62 ± 0.06
C38	2.38 ± 0.09	14.08 ± 0.37	8.61 ± 0.53
R39	0.89 ± 0.06	15.40 ± 0.61	8.19 ± 0.24
A40	3.32 ± 0.21	3.97 ± 0.15	7.44 ± 0.04

Isomerization of the disulfide bond between C14 and C38 at the active site of BPTI provides at least one mechanism for conformational exchange.[20,21] The values of τ_{ex} reported in Table 1 for C38 and R39 are in excellent agreement with exchange rates determined using an on-resonance rotating frame experiment;[20] however, the precision of the present results is approximately 10-fold greater. Results for other spins have not been reported previously. The range of exchange time constants observed vary from <0.5 ms for C14 and K15 to 4.52 ms for A16. These results suggest that the conformational exchange process is not a simple two-state disulfide isomerization. Either the time dependence of the exchange process is not well-described by a single-exponential correlation function, or multiple dynamic processes give rise to exchange effects.

In conclusion, the modified CPMG experiment compensates for evolution between in-phase and antiphase transverse coherences during the spin−echo pulse train and thereby allows quantitative measurement of conformational exchange processes on 0.5 to 5 ms time scales. Together with the off-resonance rotating frame[8,9] and zz-exchange experiments,[10−12] the new technique enables kinetic processes over biologically significant time scales from 10^{-5} s to 10^{-1} s to be investigated in macromolecules.

Supporting Information Available: Relaxation rate constants for all τ_{cp} delays and dispersion curves for residues A16, G36, G37, and A40 are available (PDF). This material is available free of charge via the Internet at http://pubs.acs.org.

JA983961A

(19) Huang, K.; Andrec, M.; Heald, S.; Blake, P.; Prestegard, J. H. *J. Biomol. NMR* **1997**, *10*, 45−52.

(20) Szyperski, T.; Luginbühl, P.; Otting, G.; Güntert, P.; Wüthrich, K. *J. Biomol. NMR* **1993**, *3*, 151−164.
(21) Otting, G.; Liepinsh, E.; Wüthrich, K. *Biochemistry* **1993**, *32*, 3571−3582.
(22) Palmer, A. G.; Cavanagh, J.; Wright, P. E.; Rance, M. *J. Magn. Reson.* **1991**, *93*, 151−170.
(23) Kay, L. E.; Keifer, P.; Saarinen, T. *J. Am. Chem. Soc.* **1992**, *114*, 10663−10665.
(24) Mosteller, F.; Tukey, J. W. *Data Analysis and Regression. A Second Course in Statistics*; Addison-Wesley: Reading, MA, 1977.